Journal of Applied Electrochemistry (2006) 36:545–556
DOI 10.1007/s10800-005-9104-9

Electrochemical behaviour of poly(pyrrole) coatings on steel

L. KOENE[1,3,*], W.J. HAMER[2] and J.H.W. DE WIT[2]
[1]*Corrosion & Antifouling, TNO Science & Industry, PO Box 505, NL-1780 AM, Den Helder, The Netherlands*
[2]*Section Surfaces & Interfaces, Department of Materials Science & Engineering, Delft University of Technology, Rotterdamseweg 137, NL-2628 AL, Delft, The Netherlands*
[3]*Current address: Engineering Mechanics, Faculty of Aerospace Engineering, Delft University of Technology, PO Box 5058, NL-2600GB, Delft, The Netherlands*
*(*author for correspondence, tel.: + 31-15-278-93-92, fax: + 31-15-261-14-65, e-mail: l.koene@tudelft.nl)*

Received 4 January 2005; accepted in revised form 24 November 2005

Key words: coatings, conducting polymer, mild steel, oxalate, poly(styrene sulfonate)

Abstract

The electrochemical and corrosion protective properties of electrochemically deposited thin films of polypyrrole (PPy) have been studied. Two systems have been investigated: (1) Oxalate-doped PPy; and (2) a dual layer system consisting of PPy-oxalate and PPy-poly(styrene sulfonate). Large anions like PSS are interesting, because they possibly prevent ingress into the layer by halide ions like chloride. Open circuit potential measurements and impedance spectra of both systems are compared. For intact coating systems the impedance spectra of the four systems investigated can be described by an equivalent circuit model consisting of an R_fQ_f circuit, due to the polypyrrole film itself, and a modified Randles circuit in series, to account for the double layer at the polypyrrole/electrolyte interface and the polypyrrole reaction. In 0.1 M NaCl the time to failure for the dual layer is almost 6-fold that of the single layer. This indicates that PSS is indeed capable of preventing the ingress of chloride ions. In 0.1 M Na_2SO_4 the time to failure for the dual layer is less than double that of the single layer.

1. Introduction

The use of heavy metals and heavy metal containing compounds, such as chromate, has to be reduced by industry for some are known to be very toxic, even carcinogenic [1] and cause great environmental damage. Suitable new alternatives are searched for and are the subject of ongoing scientific research. Interesting possibilities for coating applications are offered by conducting polymers, which have received a great deal of attention in the last three decades. In 1976 Heeger, MacDiarmid and Shirakawa and co-workers discovered conducting polymers and the ability to dope these polymers over the full conductivity range from insulators to metals [2]. Apart from fundamental interest, their unique combination of properties seems to promise a wide variety of practical applications. In 1979, Diaz and co-workers synthesised polypyrrole by electropolymerisation [3–5]. Conducting polymers, also known as synthetic metals, are considered to have technological potential to be used as coatings for corrosion protection.

Polypyrrole coatings made by electropolymerisation are often investigated on noble metals such as platinum and gold [5–8], for they allow study of the deposited layer in which electrolyte-substrate interactions as observed on commodity metals like iron and aluminium are negligible or absent. While limiting the freedom of choice in the deposition conditions, using metals such as steel and aluminium positions the research much closer to the alleged protection against corrosion. Polypyrrole has been deposited on several commodity metals [9–21]. Research has also been devoted to symmetrical systems in which the polymer serves as a membrane between two electrolytes, e.g. [22, 23].

In this work open circuit potential (OCP) measurements and impedance measurements of single layers and dual layers of PPy are investigated in two electrolytes. We have selected a mild medium, 0.10 M Na_2SO_4, and a more aggressive medium, 0.10 M NaCl. For the dual layers a second layer with large anions has been chosen, viz. poly(styrene sulfonate), for these ions probably prevent ingress of chloride into the layer [11]. Several studies indicate layers of conducting polymers to be porous, e.g. [12, 24, 25]. Water penetrates into coatings, which in the long run initiates delamination.

Impedance spectroscopy is often applied to coated systems and interpretation of impedance data at conducting polymer coatings is far from reaching consensus with many different theoretical and physical models proposed [6, 8, 26]. In addition, reproducibility of the electrodeposition of intrinsically conducting polymers is known to be a difficult issue and results between different

laboratories are not directly comparable [27, 28]. Also for this reason deposition results were examined closely.

The poor solubility of PPy (related to its conjugated structure) and its specific mechanical properties limit its applicability as a coating. There are several studies in which these properties of polypyrrole are modified by adding functional groups to the PPy ring, e.g. [29, 30]. In this study it is attempted to improve the protection against corrosion of PPy using a second (outer) layer doped with a large anion. Investigating the protection mechanism(s) of PPy layers can help us to use other synthetic metals to protect against corrosion.

It is apparent that for PPy layers a description of the formation process is important with both understanding and possible practical application in mind. In previous work, we studied the formation of PPy coatings on steel substrates [26]. Galvanostatic application of the layers was chosen to have well-defined systems.

2. Experimental

2.1. *Instrumentation and electrolytes*

Electrochemical measurements were performed with computer-controlled Solartron 1287 and 1255 equipment. The instruments were controlled using *ZPlot* and *Corrware* software from Scribner. An amplitude of 10 mV was used for the AC perturbation to measure impedance. Frequencies used range from 6.55 mHz to 65 kHz and electrolytes were made using demineralised water and p.a. chemicals.

2.2. *Formation of polypyrrole single layers*

Steel substrates of approximately 3×5 cm^2 were cut from 0.75 mm thick rolled mild steel panels obtained from Q-Panel Company of Cleveland, Ohio, USA. These panels were ground and polished down to 3 μm diamond particle size to ensure smooth and reproducible surfaces. The substrates were stored in a desiccator and used within 24 h after polishing.

The electrolyte used was an aqueous solution of 0.10 M oxalic acid (Merck) with 0.10 M pyrrole (Aldrich). The electrolyte was prepared immediately before use by adding 2080 μl of pyrrole monomer to 300 ml of 0.10 M oxalic acid solution. A working electrode area of 9 cm^2 was exposed to the electrolyte on either side of the sample. By employing a symmetrical counter-electrode configuration the electric field in the solution was kept homogeneous.

After 60 s of open circuit equilibration a current density of 1 mA cm^{-2} was applied to the sample for 1200, 3600 or 4800 s. No stirring is applied during the deposition, but the gas bubbles slowly building up at the working electrode were removed every 10 min by gentle prods. After deposition, the sample was rinsed thoroughly in water and ethanol and stored in a desiccator.

2.2.1. *Formation of polypyrrole dual layers*

The deposition of the first (inner) layer of dual layer samples was identical to the single layer procedure described above. The second (outer) layer was subsequently deposited in an aqueous solution of 0.10 M pyrrole and 5 g dm^{-3} NaPSS (Acros). The conductivity measured in this solution was 1551 μ S cm^{-1}, so a Luggin capillary was used to assure the correct measurement of the working electrode potential. The anions of the outer layer are much larger than those of the inner layer; the molecular weight of NaPSS used is about 100 000 g mol^{-1}, approximately three orders of magnitude larger than oxalate ions.

3. Results

3.1. *Polypyrrole deposition*

The galvanostatic process used for the electropolymerisation of polypyrrole has been described by several authors, e.g. Su and Iroh [31] and Nguyen Thi Le et al. [11]. The electrochemical deposition of polypyrrole is initiated by the oxidation of pyrrole monomers. This step requires a potential of approximately 1 V_{NHE}. Thus, the current supplied to the substrate initially causes the anodic dissolution of iron, for which the concurrent cathodic half reaction is the hydrogen evolution reaction (acidic environment):

$$\mathrm{Fe(s)} \leftrightarrow \mathrm{Fe^{2+}} + 2\mathrm{e^-} \tag{1}$$

$$2\mathrm{H^+} + 2\mathrm{e^-} \leftrightarrow \mathrm{H_2(g)} \tag{2}$$

For iron and steel substrates, using solutions containing oxalate ions ($C_2O_4^{2-}$) as suggested by e.g. Beck et al. [9], will temporarily protect the substrate. Given the polymerisation potential required (approx. 1 V_{NHE}) and the acidity of the solution (pH < 2), rapid dissolution of the substrate is expected to take place. The oxalates covering the substrate surface locally inhibit the anodic dissolution of iron. As a result, the (constant) electric current supplied is distributed inhomogeneously over the electrode surface. As time progresses the current will be distributed over a decreasing area, causing the electrical resistance to increase. The rise in resistance caused by the growing oxalate layer leads to a positive potential shift. Once the substrate surface is completely covered by oxalate crystals the anodic reaction is impeded, causing a dramatic increase in resistance.

The protection offered by oxalates is based upon the low (aqueous) solubility of ferrous oxalate, i.e. 0.37 mmol dm^{-3} at 18 °C [32]. As a result of this very low solubility the dissolution of iron is followed by precipitation of ferrous oxalate crystals on the substrate surface:

$$\mathrm{Fe^{2+}} + \mathrm{C_2O_4^{2-}} + 2\mathrm{H_2O} \leftrightarrow \mathrm{FeC_2O_4 \cdot [2H_2O]} \tag{3}$$

The formation of oxalate crystals enables the direct deposition of polypyrrole on iron and steel substrates, because it prevents the rapid dissolution at the polymerisation potential. Transients for 3600 s (single layer) and 4800 s (dual layer) processing time are shown in Figures 1 and 2. The time required to complete the oxalate layer, referred to as the *induction time*, varies with current density, as the oxalate deposition rate depends on the (current-driven) dissolution of iron. In this study, the induction time was practically constant as was to be expected for the current density was kept at a constant 1 mA cm^{-2}.

For each sample the deposition charge was calculated considering the end of the induction time as the starting point of polypyrrole deposition. Results are shown in Table 1. Polypyrrole layers are brittle, so a supporting nickel layer was electrodeposited on top of the polypyrrole to prevent delamination of the polymer layer during preparation of the cross-sections. Measurements of the polypyrrole layer thickness were performed on digital micrographs and are shown in Table 1. A lack of visual contrast makes it impossible to distinguish between the layers in dual layer samples. The deposition rate of the second (outer) layer was obtained by correcting the total thickness measured with the estimated thickness of the first layer. The remaining layer thickness is assumed to be entirely PSS-doped polypyrrole.

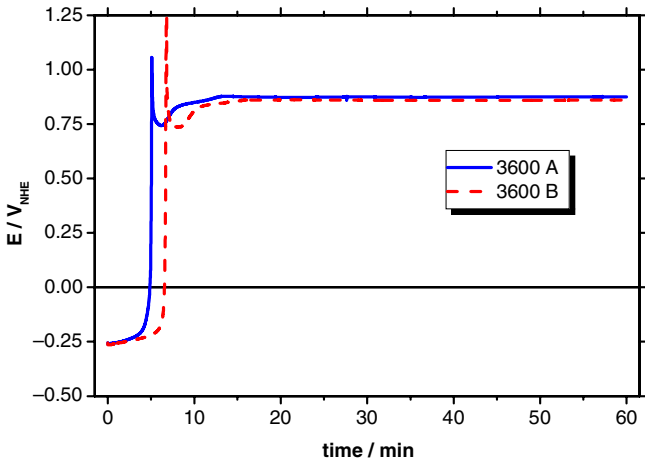

Fig. 1. Potential transients for two depositions of 3600 s in 0.1 M oxalic acid and 0.1 M pyrrole. Current density $i = 1$ mA cm^{-2}.

The rate of deposition for polypyrrole is significantly influenced by the size of the anions used [33, 34]. Deposition rates reported in the literature are listed in Table 2, together with the conditions under which they were obtained. The rates obtained in the single layer experiments are within the range of values reported in literature. The dodecyl sulphate (DDS) anions used by Tamm et al. [33] yield a similar deposition rate as the PSS anions in our experiments, even though the DDS ions are smaller than the PSS ions.

3.2. *OCP monitoring*

To investigate the corrosion protection of steel substrates by polypyrrole, the OCPs of the single layer and the dual layer coated samples were measured as a function of time. Figure 3 shows the evolution of the OCP for the PPy-oxalate coated samples in 0.10 M Na_2SO_4 and 0.10 M NaCl. In the latter, more corrosive, electrolyte, the potential immediately decreases and within about 1 day the corrosion potential of iron is reached. For the duplicate sample, exposed to 0.10 M Na_2SO_4, a nearly constant potential plateau is reached. Initially, there is a small and slow increase in potential from $+0.38$ to $+0.44$ V_{NHE}. This small increase in potential may be attributed to ion exchange of oxalates and sulphate and might also be caused by a change of activity of ions by the uptake of water by the conducting polymer film, a common process in organic coatings [36]. After about 780 h the potential in the milder electrolyte starts to decrease. Within about 4 days the potential has reached the corrosion potential of iron.

Figure 4 shows the evolution of the OCP for the PPy-oxalate-PSS coatings. In both electrolytes the layers

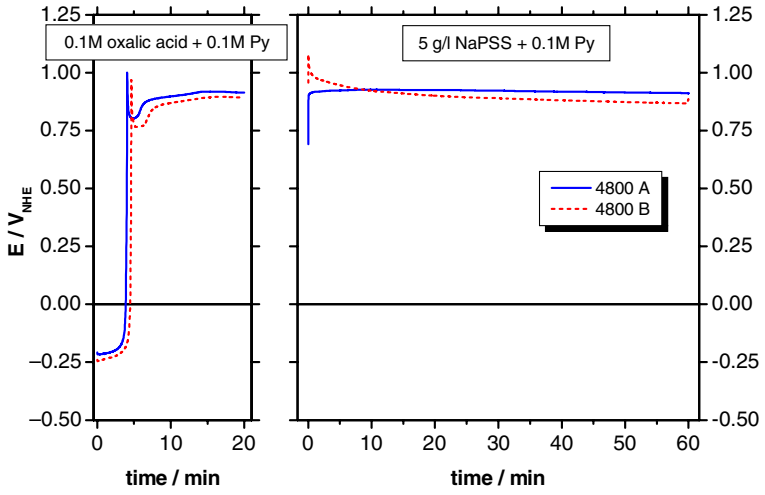

Fig. 2. Potential transients for two depositions of 4800 s in 0.1 M oxalic acid and 0.1 M pyrrole and 5 g/l NaPSS and 0.1 M pyrrole. Current density $i = 1$ mA cm^{-2}.

Table 1. Polypyrrole layer thickness (d_{PPy}), standard deviation (σ_d) and deposition rate as a function of deposition charge input

Charge input/C cm^{-2}	Processing time/s	$d_{PPy}/\mu m$	$\sigma_d/\mu m$	Deposition rate/C cm^{-2} μm^{-1}
3.3 (single)	3600	6.5	0.62	0.51
3.2 (single)	3600	6.8	0.22	0.47
4.6 (dual)	4800	26	1.05	0.18
4.5 (dual)	4800	24	0.75	0.19

Table 2. Polypyrrole deposition rates (given in C cm^{-2} μm^{-1}) in literature compared with this work

Source	Conditions	Deposition rate/C cm $^{-2}\mu m^{-1}$
Pickup et al. [35]	PPy (perchlorate) on Pt wire	0.35 ± 0.13[a]
Nguyen Thi Le et al. [11]	PPy (oxalate) on iron	0.6[b]
Diaz et al. [5]	PPy (tetrafluoroborate) on Pt	0.4
Tamm et al. [33]	PPy (small ions, generic) on Pt/Au	0.4
Tamm et al. [33]	PPy (dodecyl sulphate) on Pt/Au	0.2
This work, single layer	0.1 M oxalic acid/0.1 M pyrrole	0.48
This work, dual layer (combined)	2nd layer: 5 g/l NaPSS/0.1 M pyrrole	0.19
This work, dual layer (outer)	2nd layer: 5 g/l NaPSS/0.1 M pyrrole	0.17[c]

[a]Non-aqueous deposition in acetonitrile.
[b]Estimated maximum value: 10 μm for 6 C cm^{-2} charge input.
[c]Value calculated from corrected data.

reach an essentially constant potential plateau. In the beginning both dual layers show a small increase of the electrode potential, which can be attributed to ion exchange of oxalates and chloride or sulphate and by the uptake of water by the polypyrrole film. The potential of the dual layer sample in 0.10 M Na_2SO_4 increases from $+0.41$ to $+0.44$ V_{NHE}. The potential in 0.10 M NaCl shows an initial value of about $+0.30$ V_{NHE}, which starts to decrease slowly after 50 h. The potential reaches a new plateau at $+0.1$ V_{NHE}. A plateau at this potential has been observed and explained previously [37]. We support this explanation: the plateau is likely to be caused by the onset of pitting, which is retarded by the polypyrrole layer releasing oxalate ions that precipitate at the site of the pit [38]. After about 350 h the corrosion of the substrate can no longer be delayed by the polypyrrole layer and the potential drops to the substrate corrosion potential. After about 1100 h the layer in 0.10 M Na_2SO_4 the open circuit potential of the dual layer sample starts to decrease. Within about 50 days the potential has reached the corrosion potential of iron.

It was to be expected that the dual layer coatings protect better against corrosion than the single layer coatings [11], for the possibility of ingress of chloride in the outer layer by ion exchange is excluded. The OCP transients clearly show the influence of chloride ions in solution both for the single layer and the dual layer coatings. Ingress of chloride can take place by penetration of electrolyte solution into the coating and – for the single layer samples – by ion exchange.

As the time to failure of the polypyrrole samples the exposition time is taken when the open circuit potential has decreased halfway to the corrosion potential of iron.

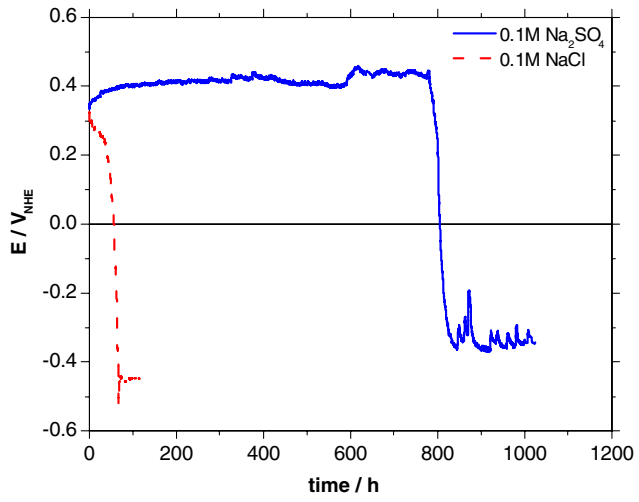

Fig. 3. Open circuit potential as a function of time for PPy/oxalate coatings in 0.1 M Na_2SO_4 and 0.1 M NaCl.

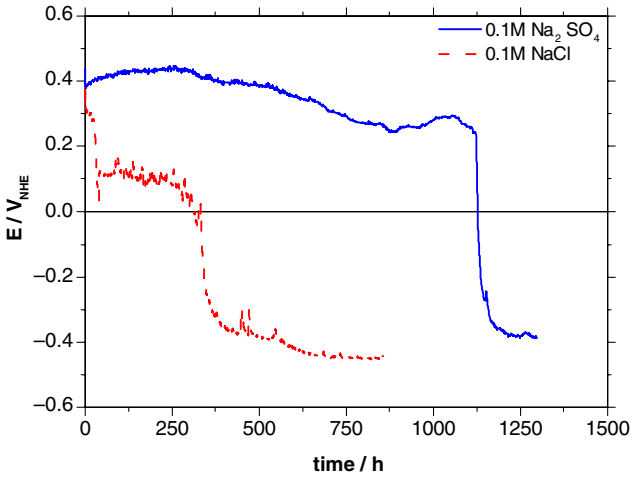

Fig. 4. Open circuit potential as a function of time for PPy/oxalate + PPy/PSS coatings in 0.1 M Na_2SO_4 and 0.1 M NaCl

These times are shown in Table 3 for the single and dual layer samples in Na_2SO_4 and NaCl. It is clear that the protection time for the dual layers is higher.

3.3. *Overview of EIS measurements*

Figures 5–8 show Nyquist plots of impedance spectra for single layer and dual layer samples immersed in 0.10 M NaCl and 0.10 M Na_2SO_4 at several times after immersion. In our opinion for systems investigated here Nyquist plots reflect the characteristics of the systems and changes therein better than Bode plots. The frequencies used in these plots range from 65 kHz to 6.5 mHz (with the exception of the $t = 0$ h measurements which range from 65 kHz to 655 mHz). Immersion times are given relative to the time to failure (%t_f). The plots show that the electrochemical behaviour of the examined systems changes drastically with time. In general, the value of the impedance at low frequencies decreases with time. Both OCP and EIS measurements show the coating was damaged. This is not surprising for on all samples blisters were observed after the coatings had failed during immersion.

4. Discussion

4.1. *Open circuit potential monitoring*

In contrast with conventional barrier coatings, intrinsically conducting polymer coatings are electrochemically active. Polypyrrole is deposited in an oxidised state, doped with an anion (A^-) to maintain charge neutrality. The electrochemical activity of polypyrrole consists of the reduction reaction of the polymer:

$$PPy^+A^- + e^- \leftrightarrow PPy^0 + A^-(aq) \quad (4)$$

The reduction potential of this reaction is approximately $+0.40\ V_{NHE}$. At steel the anodic dissolution of iron occurs:

$$Fe \leftrightarrow Fe^{2+} + 2e^- \quad (5)$$

This reaction has a standard potential of $-0.447\ V_{NHE}$. The open circuit potential of polypyrrole-coated steel is a mixed potential of the electrochemical reactions at the interface, possibly including both Equations 4 and 5. Because of the large potential difference between these reactions OCP monitoring can provide information about the dominant electrochemical process at the working electrode.

Table 3. The time to failure t_f for the single and dual layer samples in 0.1 M Na_2SO_4 and 0.1 M NaCl

Sample	t_f/h
Single layer/0.1 M Na_2SO_4	806
Single layer/0.1 M NaCl	59
dual layer /0.1 M Na_2SO_4	1125
dual layer /0.1 M NaCl	341

The results shown in Figures 3 and 4 show that chloride ions dramatically reduce the duration of polypyrrole corrosion protection. However, the potential of

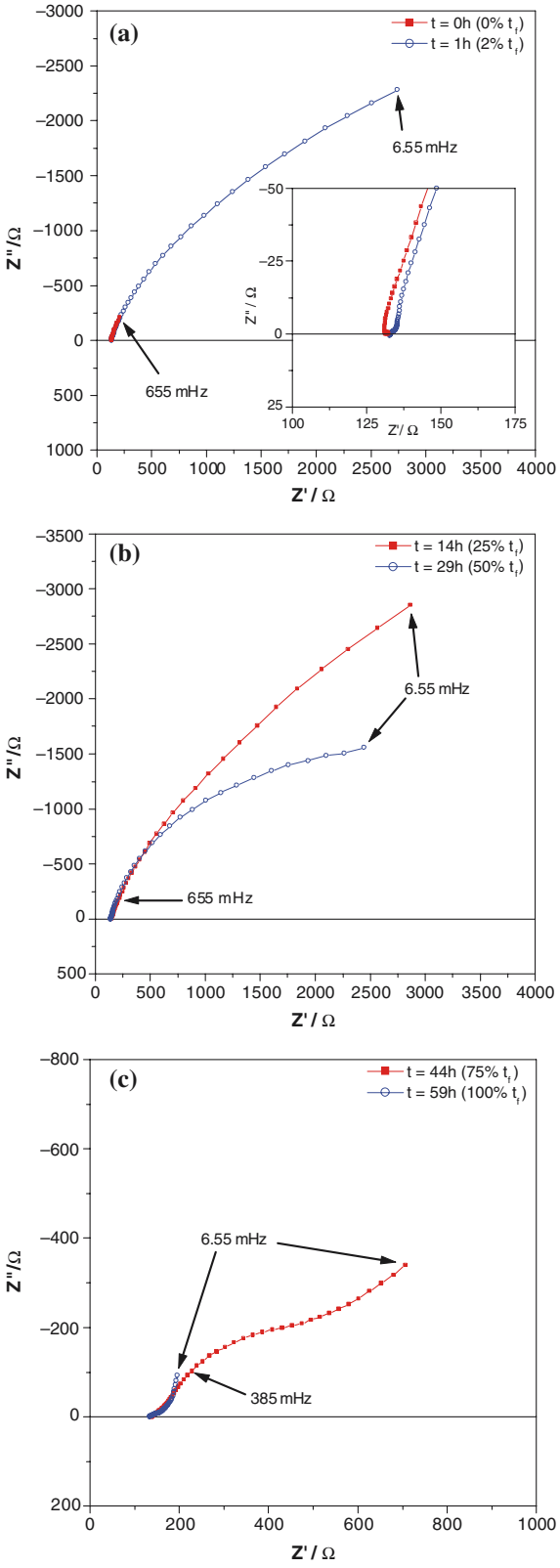

Fig. 5. Nyquist plots of impedance spectra of PPy/oxalate coated steel in 0.1 M NaCl for (a) $t = 0$ and 1 h, (b) $t = 14$ and 29 h, and (c) $t = 44$ and 59 h. Immersion times indicated both in hours and in % of time to failure t_f.

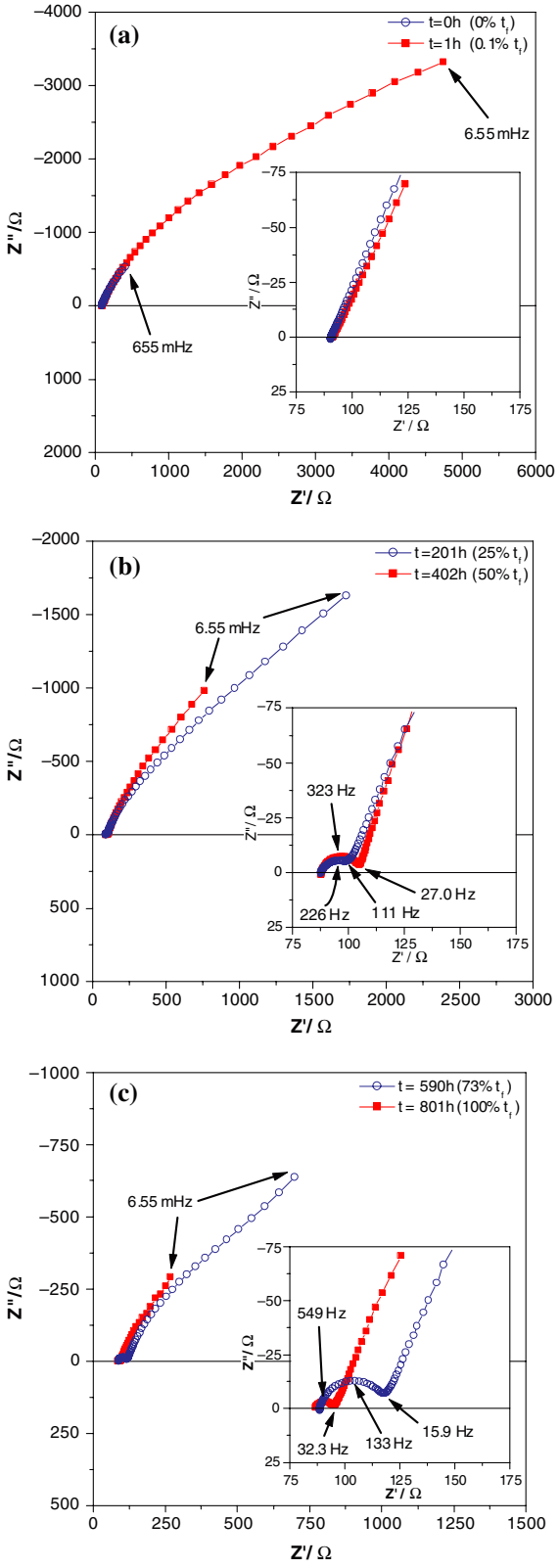

Fig. 6. Nyquist plots of impedance spectra of PPy/oxalate coated steel in 0.1 M Na_2SO_4 for (a) $t = 0$ h, (b) $t = 201$ and 403 h, and (c) $t = 590$ and 801 h. Immersion times indicated both in hours and in % of time to failure t_f.

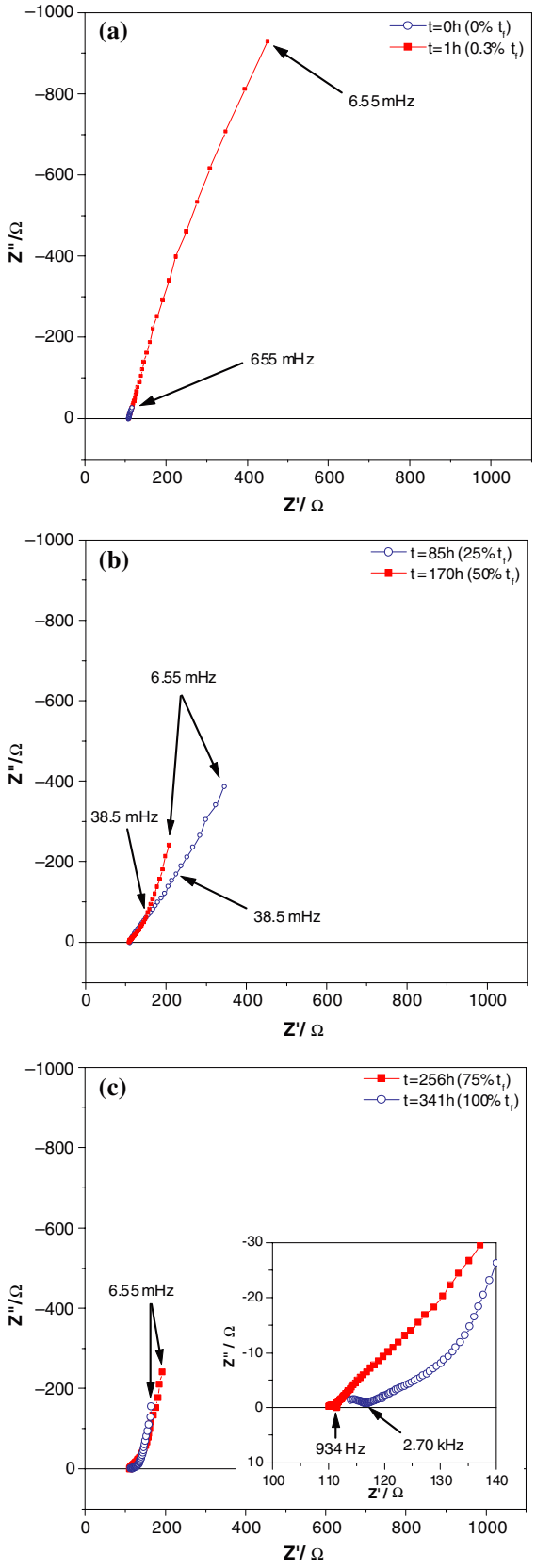

Fig. 7. Nyquist plots of impedance spectra of PPy/oxalate + PPy/PSS coated steel in 0.1 M NaCl for (a) $t = 0$ h and 1 h, (b) $t = 85$ and 170 h, and (c) $t = 256$ and 341 h. Immersion times indicated both in hours and in % of time to failure t_f.

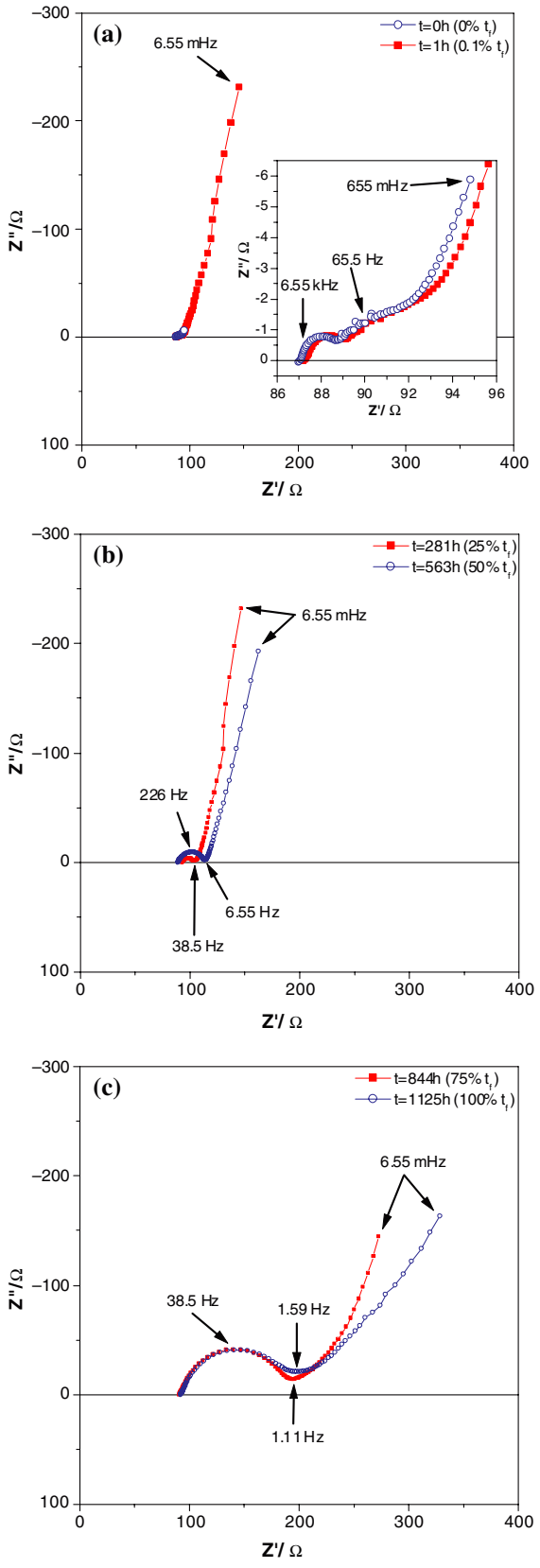

Fig. 8. Nyquist plots of impedance spectra of PPy/oxalate + PPy/PSS coated steel in 0.1 M Na_2SO_4 for (a) $t = 0$ and 1 h, (b) $t = 281$ and 563 h, and (c) $t = 844$ and 1125 h. Immersion times indicated both in hours and in % of time to failure t_f.

polypyrrole is maintained for about 1100 h by the dual layer (Figure 4), which strongly suggests that the ingress of chloride ions is impaired by the PSS anions of the outer layer.

Figure 3 shows comparable results as obtained by Nguyen Thi Le et al. [37]. However, in our experiments only two "plateaus" are observed, instead of three [37]. According to Nguyen Thi Le et al. the plateaus in the OCP transients represent the passivity breakdown of polypyrrole-coated iron, comparable to the passivity breakdown of iron substrates. They state that the first (most anodic) plateau corresponds to the formal potential of polypyrrole. Further, the decrease of the potential over time is explained by the reduction of polypyrrole supporting the oxidation of iron to sustain the protective iron oxide layer.

The polypyrrole/NaPSS dual layer coated samples were immersed using the same conditions as in the single layer systems, i.e. 0.10 M NaCl and 0.10 M Na_2SO_4. OCP transients for dual layer experiments are shown in Figure 4. The curves exhibit behaviour that is somewhat similar to that of the single layer systems while the time to failure is significantly improved. Again, the potential observed in 0.10 M Na_2SO_4 rises slightly before the system fails.

4.2. *Impedance*

4.2.1. *Physical model of the sample interface*

In the absence of a redox couple in solution, for an intact coating system consisting of an electroactive conducting polymer electrodeposited on a metal, one can expect the following contributions to its impedance:

- An iron oxide layer between the metal and the conducting polymer film.
- Charge transport within the conducting polymer film: electrons, anions, cations, and holes.
- The reduction of polypyrrole involving a charge transfer reaction (Faraday reaction) and diffusion of reactants.
- The electrochemical double layer at the polymer film.

A metal oxide layer is often described by a Voigt element that can be represented by a resistance and capacitance in parallel. The same model can be used for the polymer film. The Faraday reaction can be represented by a ionic charge transfer resistance and a Warburg impedance to model the anion diffusion from the conducting polymer. The double layer at the polymer film can be represented by a capacitance. Thus, the following elements are to be expected in an the equivalent circuit model: R_{mf} the resistance of the oxide layer between the polymer film and the metal; C_{mf} the capacitance in parallel; R_f the resistance of the polymer film proper; C_f is the capacitance in parallel; R_{ct} the charge transfer resistance of the pyrrole reaction; W the

Warburg impedance; and C_d the double layer capacitance associated with the polypyrrole/solution interface.

A theoretical model as described above was proposed by Vorotyntsev et al. [39]. A similar model, however without a contribution of a metal oxide layer or charge transfer resistance between metal and film, was proposed by Brillas et al. [40]. The physical model used by Krstajiæ et al. [12] is different: in their model iron dissolution takes place through pores. Based on dc measurements and experiments with PPy/Pt we think this does not occur in our system, at least not at the start of exposition to the electrolyte solutions. However, in the impedance model one has to account for the inhomogeneity of the polypyrrole coating layer. As a consequence constant phase elements (with symbol Q) have to be introduced to describe the non-ideal behaviour of capacitative elements involved. The same holds for the diffusion from the polypyrrole film. This created the overall equivalent circuit model shown in Figure 9.

4.2.2. *Contribution of the polypyrrole layer*

Only one semi-circle was found in the higher frequency region. Nyquist plots of impedance spectra show similar behaviour as observed by Beck et al. [9] at a 3 μm polypyrrole (oxalate) layer on iron in 0.1 M $H_2C_2O_4$ (aq). The diameter of the semicircle observed at high frequencies corresponds to a small R_f-value up to about $6\Omega cm^2$ in the initial phase of exposition to 0.10 M NaCl or 0.10 M Na_2SO_4 (see Table 4). Beck et al. attribute this small semicircle to a porous iron(II) oxalate interlayer. We think the small semi-circle in the impedance spectra at high frequencies should be attributed to the conducting polymer coating. We will justify this below. The conductivity κ is defined by the equation:

$$\kappa = \frac{d_{PPy}}{R_f} \tag{6}$$

For the dual layers, the initial R_f-values are $4 \pm 2\Omega cm^2$ and the thickness is 23.5 μm. Thus the initial conductivity of the dual layers is about 0.6 mS cm^{-1}. For the single layers, the initial R_f-values is are about 1Ω cm^2 (or lower) and their thickness is 8 μm. Thus the conductivity of the single layers is about 0.6 mS cm^{-1} (or higher). These figures are the same order of magnitude as is found by Beck et al. [9] and Nguyen Thi Le et al. [37], respectively, 0.3 and 0.4 mS cm^{-1}. Su and Iroh [41] have found that no iron(II) oxalate layer remains after deposition of polypyrrole. Consequently, the small semi-circle in the impedance spectra at high frequencies should be attributed to the conducting polymer coatings and not to an iron(II) oxalate interlayer as proposed by Beck et al. [9]. Polypyrrole layers are porous, and so a part of the conductivity observed may be due to electrolyte, which has penetrated into the polypyrrole coating. The data strongly suggest that the contribution due to R_{mf} and Q_{mf} is negligible. Nguyen Thi Le et al. [37] have performed experiments using a metal | PPy | metal arrangement which provided further evidence for this hypothesis.

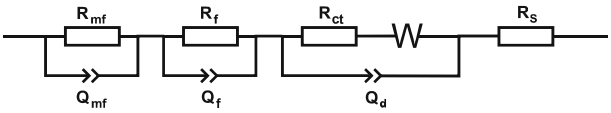

Fig. 9. Equivalent circuit model. For the meaning of its elements see text.

Table 4. Initial values for R_f, the resistance of the polymer coating, for the single and dual layer coatings in 0.1 M NaCl and 0.1 M Na_2SO_4

Sample	R_f/Ω cm^2	$d_{Ppy}/\mu m$
Single layer/0.1 M NaCl	1.0	8
Single layer/0.1 M Na_2SO_4	0	8
Dual layer/0.1 M NaCl	5.8	24
Dual layer/0.1 M Na_2SO_4	2.2	26

4.2.3. *Polypyrrole redox reaction*

The part of the model describing the redox reaction and the double layer at the polypyrrole/electrolyte interface contains a Faraday contribution due to the polypyrrole reaction (equation 4) and a double layer contribution. To model the double layer a constant phase element (CPE) is used to account for the non-homogeneity of the interface [42]:

$$Z_{cpe} = \frac{1}{Y_0(j\omega)^n} \tag{7}$$

In this equation $j = \sqrt{-1}$, $0 < n \leq 1$ and Y_0 is a constant with the dimension F cm^{-2} s^{n-1}. To describe the behaviour of impedance spectra at low frequencies an exponent α is introduced in the expression for the Warburg impedance. Several models and expressions are used to describe this characteristic behaviour of conducting polymers, e.g. [37, 43, 44]. The finite-length Warburg impedance used here is expressed by ([42, 45]):

$$W_o = R_W \frac{\coth(j\omega s)^\alpha}{(j\omega s)^\alpha} \tag{8}$$

In this equation $s = \lambda^2/D$ [42] where λ is the effective diffusion thickness and D the effective diffusion coefficient of the particles (oxalate ions in this case). This model for the polypyrrole reaction at a polypyrrole electrode in the absence of another electrochemical reaction (i.e. intact coating) is a modified Randles circuit model.

4.2.4. *Impedance data analysis*

The impedance data were analysed by NLLS-fitting of equivalent circuits to the data. The conduction of charges within the polypyrrole layer contributing to the high-frequency part of the data (section 4.2.2) is excluded from the discussion in this section.

4.2.4.1. *Single layer systems.* The single layer data in Table 5 have been fitted using a $R_S(RQ)$ equivalent circuit. This is a simple phenomenological model, in which R_S is the ohmic resistance of the system. Although charge transfer, double layer and diffusion are considered, the processes cannot be separated from each other

Table 5. Values for the parameters of the $R(RQ)$ circuit obtained from the best NLLS fit to the impedance data. Data for *single layer* (PPy/oxalate) samples at different t_f fractions

	$\%t_f$	E_{OCP}/V_{NHE}	$R_S/\Omega\ cm^2$	$R/\Omega\ cm^2$	Q		χ^2
					n	$Y_0/F\ cm^{-2}\ s^{n-1}$	
0.1 M NaCl	0.1	+0.390	135	5.3×10^3	0.80	1.8×10^{-3}	5.7×10^{-3}
	25	+0.435	143	8.0×10^3	0.76	1.9×10^{-3}	1.6×10^{-3}
	50	+0.366	141	3.7×10^3	0.83	2.2×10^{-3}	8.1×10^{-3}
	75	+0.271	139	1.4×10^3	0.53	4.3×10^{-3}	5.9×10^{-3}
	100	+0.102	128	–	0.33	2.3×10^{-2}	2.6×10^{-2}
0.1 M Na_2SO_4	0.1	+0.349	90.3	9.2×10^3	0.70	7.2×10^{-4}	9.8×10^{-4}
	25	+0.413	94.3	5.5×10^3	0.69	2.7×10^{-3}	1.0×10^{-3}
	50	+0.415	103	4.3×10^3	0.77	8.3×10^{-3}	1.7×10^{-4}
	75	+0.432	131	3.0×10^3	0.85	1.4×10^{-2}	8.7×10^{-4}
	100	+0.201	95.1	1.3×10^3	0.76	2.9×10^{-2}	7.3×10^{-5}

because they occur in overlapping frequency ranges. The NaCl parameters in Table 5 indicate that diffusion becomes increasingly dominant as for the CPE power (n) decreases from more capacitative to diffusive values, while for Na_2SO_4 the values of the CPE power (n) remain double layer like.

4.2.4.2. *Dual layer systems*. The results of the fits to the dual layer systems in Table 6 show some remarkable differences between NaCl and Na_2SO_4 immersions. The fits describe the impedance data adequately over each decade of the frequency range. In NaCl the charge transfer resistance is negligible relative to the Warburg diffusion resistance. Initially, the dual layer system immersed in NaCl behaves capacitatively and shows finite-length diffusion transport.

In Na_2SO_4, the dual layer system shows an increase in charge transfer resistance (R_{ct}) with time. The increasing charge transfer resistance is visible in Figure 8 as the diameter of the semi-circle at higher frequency increases with time. This may be related to the reduction of polypyrrole as the subsequent loss of available charge transfer sites at the polypyrrole/solution interface will increase R_{ct}.

A transition from finite-length diffusion to semi-infinite diffusion is apparent from the Nyquist plots in Figures 6 and 8. This strongly suggests that ion diffusion in solution slowly replaces charge diffusion within the polypyrrole layer as the dominant charge transfer process as the slope of the low-frequency part in the Nyquist plot approaches 45° near $t = t_f$. The simultaneous increase in R_{ct} and R_W indicates that the reaction rate of the system's Faradaic process decreases with time.

4.3. *Failure mechanism of polypyrrole layers on steel*

4.3.1. *Introductory remarks*

Above it was assumed that the polypyrrole layer on steel fails when the open circuit potential shows a significant drop. Following that assumption, one would expect a coincident transition in the impedance spectra shown in Figures 5–8. However, the transition from predominantly polypyrrole redox behaviour to predominantly iron dissolution does not appear as clearly in the Nyquist plots. If the polypyrrole layers were non-conductive, the substrate electrochemistry would only be measurable if the coating had physically failed (i.e. it is punctured). Since the polypyrrole coating is conductive it does not have to be damaged to reveal processes underneath the coating/solution interface.

The time to failure or protection time of all samples is rather modest. This is also the case for similar polypyrrole systems [37, 46]. Polypyrrole systems have a high porosity for which we expect a high water uptake. In their oxidised form polypyrrole layers are hydrophilic [47, 48]. It is likely that local regions are formed with water between the hydrophilic polypyrrole layer and the metal substrate. When this occurs dissolution of iron is expected.

Table 6. Values for the parameters of the modified Randles part obtained from the best NLLS-fit to the impedance data. Data for *dual layer* (PPy/oxalate + PPy/PSS) samples at different t_f fractions

	$\%t_f$	E_{OCP}/V_{NHE}	$R_{ct}/\Omega\ cm^2$	Q		W_o			χ^2
				n	$Y_0/F\ cm^{-2}\ s^{n-1}$	$R_W/\Omega\ cm^2$	s/s	α	
0.1 M NaCl $R(W_oQ)$ model	0.3	+0.335	–	1.0	6.51×10^{-3}	49.0	0.322	0.37	5.2×10^{-5}
	25	+0.121	–	0.80	1.01×10^{-2}	347	10.4	0.33	6.0×10^{-6}
	50	+0.069	–	0.76	1.18×10^{-2}	143	8.25	0.41	1.2×10^{-5}
	75	+0.109	–	0.72	8.49×10^{-3}	117	7.75	0.44	2.1×10^{-5}
	100	−0.190	–	0.48	3.30×10^{-10}	60.4	8.35	0.44	8.0×10^{-5}
0.1 M Na_2SO_4 $R((RW_o)Q)$ model	0.1	+0.390	2.74	0.64	1.05×10^{-3}	14.3	0.838	0.41	2.4×10^{-4}
	25	+0.435	9.94	0.79	1.08×10^{-4}	13.9	0.937	0.43	1.4×10^{-4}
	50	+0.366	22.8	0.84	8.21×10^{-5}	9.60	0.684	0.41	1.3×10^{-4}
	75	+0.271	91.2	0.89	7.25×10^{-5}	53.5	4.41	0.31	5.1×10^{-4}
	100	+0.102	81.4	0.89	8.87×10^{-5}	101	6.29	0.28	3.8×10^{-4}

4.3.2. *Sodium chloride environment*

Figure 5 shows Nyquist plots recorded for a single layer system immersed in NaCl. The plots show a distinct drop in the overall impedance around t_f. Throughout the immersion time, the low-frequency phase angle of 40–60° indicates semi-infinite Warburg behaviour. Transfer of charges between solution and polymer is possible, allowing chloride ions to enter the polymer layer and ultimately access the substrate surface. This access of corrosive ions is reflected in the time to failure t_f; after a little over 2 days the observed potential reaches the corrosion potential of the substrate.

In contrast, the dual layer system in sodium chloride behaves differently (see Figure 7). This system shows finite-length Warburg diffusion (Equation 8). This "blocking" behaviour continues after the time has passed 100% t_f. Characteristic for conducting polymer transport properties, the finite-length diffusion behaviour is indicative of an intact polypyrrole layer [49, 50] at $t \geq t_f$. At the same time, the drop in potential indicates corrosion activity that can occur beneath a coating. The corrosion products underneath the coating will eventually cause the blister to break, which is evidenced by the disappearance of the finite-length Warburg behaviour at $t = 150\%\ t_f$ [51].

Figure 10 shows the evolution of the low-frequency resistance R_{LF} for both single and dual layer samples in NaCl and Na_2SO_4. The values plotted represent the real part of the complex impedance data measured at a frequency of 6.55 mHz. The curves for NaCl both show a drop in R_{LF} up to the time of failure, after which they rise again. In the single layer sample, ion exchange may occur as oxalate ions are replaced by chloride ions. Since chloride ions are smaller this may result in a higher mobility of charge carriers in the polymer, causing a decrease in R_{LF}. In the dual layer sample PSS anions cannot be exchanged because of their size. However, the reduction of the polymer causes ingress of cations from the solution to maintain charge neutrality. The additional (cat)ions may also increase the conductivity of the coating. Thus, the low-frequency conduction in these coatings may be attributed to mobile charges in the polymer backbone and to the mobile cations they contain. The rise in R_{LF} after the time to failure may be explained by the build-up of corrosion products, which pose an increased charge transfer barrier visible at low frequencies.

4.3.3. *Sodium sulphate environment*

Figures 6 and 8 show Nyquist plots of single and dual layer samples immersed in 0.10 M Na_2SO_4 solutions. The single layer experiment shows semi-infinite Warburg behaviour throughout, indicated by the 40–60° low frequency phase angle. In the high frequency range the development of an additional charge transfer process is visible, possibly the onset of substrate corrosion reactions. The magnitude of the impedance curves in Figure 6 decreases with time, indicating that overall conduction in the system increases significantly. This increase is also apparent in Figure 10. Analogous to the behaviour of the single layer sample in NaCl environment, this may be attributed to ingress of electrolyte ions. After t_f the single layer sample shows an increase in R_{LF}. Although decisively less corrosive than the sodium chloride environment, sodium sulphate may cause the substrate to corrode. This is evidenced by the build-up of corrosion products on the substrate, which has been confirmed by visual inspection of the sample after immersion. These corrosion products cause the diffusion of charge carriers to be hindered, resulting in an increase in R_{LF}.

The right panel in Figure 10 also shows the evolution of R_{LF} for a dual layer sample immersed in Na_2SO_4 (○ symbols). The time to failure t_f is clearly marked by a distinct drop in R_{LF}. Before t_f the low-frequency resistance gradually rises, possibly caused by polymer reduction. Nyquist plots in Figures 8 show that the finite-length Warburg behaviour initially observed changes into semi-infinite Warburg behaviour between 60 and 80% t_f [51]. This cannot be explained by further

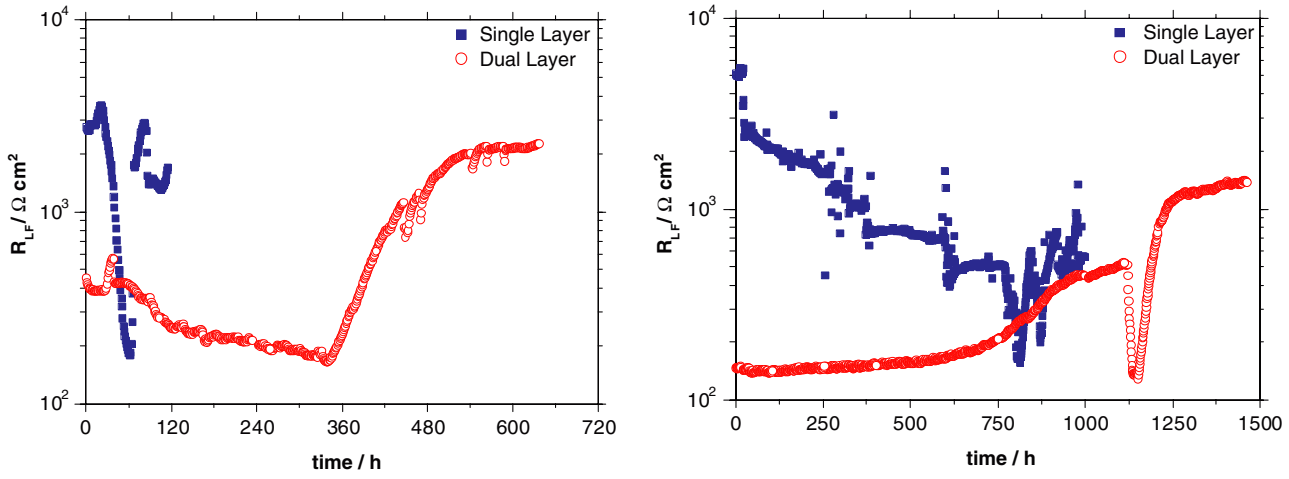

Fig. 10. Low-frequency resistance R_{LF} of single and dual layer samples in 0.1 M NaCl sodium chloride (left) and 0.1 M Na_2SO_4 (right). Values plotted represent the real component of the complex impedance data measured at 6.55 mHz.

(or even complete) reduction of the polymer, because this requires electrochemical potentials well below the observed 200–300 mV_{NHE} [50].

The rise in R_{LF} after t_f may be explained by the build-up of corrosion products, as in sodium chloride environment.

5. Conclusions

The use of large anions instead of oxalate ions has a significant effect on the deposition rate of polypyrrole. The lower rate for PSS anions may be explained by the additional volume taken up by their size compared to oxalate. The rate of consumption of pyrrole monomers is not expected to change, as it depends on the current density.

In general the impedance spectra of the four systems investigated can be described by a model consisting of an R_fQ_f circuit, due to the polypyrrole film, and a modified Randles circuit in series to account for the double layer at the polypyrrole/electrolyte interface and the polypyrrole reaction. For intact coating systems the contribution of an iron oxide layer between the coating film and the steel substrate, if present, is negligible. In 0.10 M NaCl the time to failure for the dual layer is almost sixfold that of the single layer. This indicates that the use of PSS ions indeed help to prevent the ingress of chloride ions. In 0.10 M Na_2SO_4 the time to failure for the dual layer is less than double that of the single layer.

The uptake of electrolyte by the porous polypyrrole coatings is probably most important. It explains why the protection time of samples investigated is low. Water between the coating and the metal causes delamination. The protection time of the dual layer coatings can be improved by using other large anions and refined process conditions [52]. Another interesting possibility is attempting to seal the polypyrrole pores. This may be achieved by making composite coatings of (modified) polypyrrole and one or more environmentally friendly oxides.

Acknowledgements

SenterNovem/IOP Heavy Metals & Environmental Technology Research Fund financially supported this research under project number izw98101.

References

1. M. Costa, *Toxicol. Appl. Pharmacol.* **188** (2003) 1.
2. A.J. Heeger, *Curr. Appl. Phys.* **1** (2001) 247.
3. A.F. Diaz and K.K. Kanazawa, *J. Chem. Soc. Chem. Commun.* (1979) 635.
4. K.K. Kanazawa, A.F. Diaz, R.H. Geiss, W.D. Gill, J.F. Kwak, J.A. Logan, J.F. Rabolt and G.B. Street, *J. Chem. Soc. Chem. Commun.* (1979) 854.
5. A.F. Diaz, J.I. Castillo, J.A. Logan and W.Y. Lee, *J. Electroan. Chem.* **129** (1981) 115.
6. D.L. Miller and J.O'M. Bockris, *J. Electrochem. Soc.* **139** (1992) 967.
7. A. Alumaa, A. Hallik, U. Mäeorg, V. Sammelselg and J. Tamm, *Electrochim. Acta* **49** (2004) 1767.
8. U. Rammelt, S. Bisschoff, M. El-Dessouki, R. Schulze, W. Plieth and L. Dunsch, *J. Solid State Electrochem.* **3** (2000) 406.
9. F. Beck, R. Michaelis, F. Schloten and B. Zinger, *Electrochim. Acta* **39** (1994) 229.
10. B. Garcia, A. Lamzoudi, F. Pillier, H. Nguyen Thi Le and C. Deslouis, *J. Electrochem. Soc.* **149** (2002) B560.
11. H. NguyenThi Le, B. Garcia, C. Deslouis and Q. Le Xuan, *J. Appl. Electrochem.* **32** (2002) 105.
12. N.V. Krstajić, B.N. Grgur, S.M. Jovanović and M.V. Vojnović, *Electrochim. Acta* **42** (1997) 1685.
13. A. de Bruyne, J.L. Delplancke and R. Winand, *J. Appl. Electrochem.* **27** (1997) 867.
14. D.W. DeBerry, *J. Electrochem. Soc.* **132** (1982) 1022.
15. M.A. Malik, M.T. Galkowski, H. Bala, B. Grzybowska and P.J. Kuleska, *Electrochim. Acta* **44** (1999) 2157.
16. W.C. Su and J.O. Iroh, *Electrochim. Acta* **42** (1997) 2685.
17. J. He, V.J. Gelling, D.E. Tallman, G.P. Bierwagen and G.G. Wallace, *J. Electrochem. Soc.* **147** (2000) 3667.
18. V.J. Gelling, M.M. Wiest, D.E. Tallman, G.P. Bierwagen and G.G. Wallace, *Progr. Org. Coatings* **43** (2001) 149.
19. S.B. Saidman and J.B. Bessone, *J. Electroan. Chem.* **521** (2002) 87.
20. V.T. Truong, P.K. Lai, B.T. Moore, R.F. Muscat and M.S. Russo, *Synth. Metals* **110** (2000) 7.
21. Y.F. Jiang, X.W. Guo, Y.H. Wei, C.Q. Zhai and W.J. Ding, *Synth. Metals* **139** (2003) 335.
22. C. Deslouis, M.M. Musiani, B. Tribollet and M.A. Vorotyntsev, *J. Electrochem. Soc.* **142** (1995) 1902.
23. R.H.J. Schmitz and K. Jüttner, *Electrochim. Acta* **44** (1999) 1627.
24. F.T.A. Vork and L.J.J. Janssen, *Electrochim. Acta* **33** (1988) 1513.
25. G. Garcia-Belmonte, *Electrochem. Comm.* **5** (2003) 236.
26. W.J. Hamer, L. Koene and J.H.W. de Wit, *Mater.Corr.* **55** (2004) 653.
27. P.G. Pickup. Electrochemistry of electronically conducting polymer films, *in* R.E. White, J.O'M. Brockris and B.E. Conway (Eds), Modern Aspects of Electrochemistry Vol. 33, (Kluwer Academic/Plenum Publishers, New York, 1999), pp. 549–597.
28. U. Barsch, F. Beck, G. Hambitzer, R. Holze, J. Lippe and I. Stassan, *J. Electroan. Chem.* **369** (1994) 97.
29. V. Haase and F. Beck, *Electrochim. Acta* **39** (1994) 1195.
30. J.-Y. Lee and S.-M. Park, *J. Electrochem. Soc.* **147** (2000) 4189.
31. W.C. Su and J.O. Iroh, *J. Appl. Polym. Sci.* **65** (1997) 617.
32. T. Biestek and J. Weber, *Electrolytic and Chemical Conversion Coatings: A Concise Survey of their Production, Properties and Testing* (Portcullis Press, Redhill, 1976).
33. J. Tamm, A. Alumaa, A. Hallik, U. Johanson, L. Tamm and T. Tamm, *Russ. J. Electrochem.* **38** (2002) 182.
34. S.B. Saidman, *Electrochim. Acta* **48** (2003) 1717.
35. P.G. Pickup and G.L. Duffitt, *J. Chem. Soc. Faraday Trans.* **88** (1992) 1417.
36. E.P.M. van Westing, '*Determination of Coating Performance with Impedance Measurements*', Dissertation (Delft University of Technology, Delft, 1992).
37. H. Nguyen Thi Le, B. Garcia, C. Deslouis and Q. Le Quan, *Electrochim. Acta* **46** (2001) 4259.
38. H. Nguyen Thi Le, M.C. Bernard, B. Garcia-Renaud and C. Deslouis, *Synth. Metals* **140** (2004) 287.
39. M.A. Vorotyntsev, J.P. Badiali and E. Vieil, *Electrochim. Acta* **41** (1996) 1375.
40. E. Brillas, J. Carrasco, V. Fernandaz, J.A. Garrido, R.M. Rodriguez, P.L. Cabot, E. Perez and F. Centellas, *Synth. Metals* **101** (1999) 24.
41. W. Su and J.O. Iroh, *Electrochim. Acta* **46** (2000) 1.
42. J. Ross Macdonald, *Impedance Spectroscopy: Emphasizing Solid Materials and Systems* (John Wiley & Sons, New York, 1987).

43. M.J. Rodriguez Presa, R.I. Tucceri, M.I. Florit and D. Posadas, *J. Electroan. Chem.* **502** (2001) 82.
44. J.-Y. Lee and S.-M. Park, *J. Electrochem. Soc.* **147** (2000) 4189.
45. R. Cabanel, R. Barral, J.-P. Diard, B. Le Gorrec and C. Montella, *J. Appl. Electrochem.* **23** (1993) 93.
46. B.N. Grgur, N.V. Krstajić, M.V. Vojnović, Č. Lačnjevac and Lj. Gajić-Krstajić, *Progr. Org. Coatings* **33** (1998) 1.
47. Y.-C. Liu and B.-J. Hwang, *J. Electroan. Chem.* **501** (2001) 100.
48. U. Rammelt, P.T. Nguyen and W. Plieth, *Electrochim. Acta* **48** (2003) 1257.
49. G. Garcia-Belmonte and J. Bisquert, *Electrochim. Acta* **47** (2002) 4263.
50. M.E.G. Lyons, Charge percolation, in M.E.G. Lyons (ed.), '*Electroactive Polymers in Electroactive Polymer Electrochemistry', Part 1 – Fundamentals*, (Plenum Press, New York, 1994) pp. 1–226.
51. W.J. Hamer, '*Polypyrrole Electrochemistry: Environmentally Friendly Corrosion Protection of Steel: (im)possibilities*', Dissertation, (Delft University of Technology, Delft, 2005).
52. N.T.L. Hien, B. Garcia, A. Pailleret and C. Deslouis, *Electrochim. Acta* **50** (2005) 1747.